J|A|C|S
ARTICLES
Published on Web 09/21/2004

Characterization of Nonspecific Protein−DNA Interactions by ^{1}H Paramagnetic Relaxation Enhancement

Junji Iwahara,[†] Charles D. Schwieters,[‡] and G. Marius Clore*,[†]

Contribution from the Laboratory of Chemical Physics, National Institute of Diabetes and Digestive and Kidney Disease, National Institutes of Health, Bethesda, Maryland 20892-0520 and the Division of Computational Bioscience, Center for Information Technology, National Institutes of Health, Bethesda, Maryland 20892-5624

Received June 24, 2004; E-mail: mariusc@intra.niddk.nih.gov

Abstract: Nonspecific protein−DNA interactions play an important role in a variety of contexts related to DNA packaging, nucleoprotein complex formation, and gene regulation. Biophysical characterization of nonspecific protein−DNA interactions at the atomic level poses significant challenges owing to the dynamic nature of such complexes. Although NMR spectroscopy represents a powerful tool for the analysis of dynamic systems, conventional NMR techniques have provided little information on nonspecific protein−DNA interactions. We show that intermolecular ^{1}H paramagnetic relaxation enhancement (PRE) arising from Mn^{2+} chelated to an EDTA-group covalently attached to a thymine base (dT-EDTA-Mn^{2+}) in DNA provides a unique approach for probing the global dynamics and equilibrium distribution of nonspecific protein−DNA interactions. For nonspecific DNA binding, similar intermolecular ^{1}H−PRE profiles are observed on the ^{1}H resonances of the bound protein when dT-EDTA-Mn^{2+} is located at either end of a DNA oligonucleotide duplex. We demonstrate the applicability of this approach to HMG-box proteins and contrast the results obtained for nonspecific DNA binding of the A-box of HMGB-1 (HMGB-1A) with sequence-specific DNA binding of the related SRY protein. Intermolecular ^{1}H-PRE data demonstrate unambiguously that HMGB-1A binds to multiple sites in multiple orientations even on a DNA fragment as short as 14 base pairs. Combining the ^{1}H-PRE data with the crystal structure of the HMGB-1 A-box/cisplatin-modified DNA complex allows one to obtain a semiquantitative estimate of the equilibrium populations at the various sites.

Introduction

Nonspecific protein−DNA interactions generally involve a highly dynamic process in which a protein can bind to and readily move between multiple overlapping binding sites on the DNA with comparable affinity. All DNA binding proteins are capable of nonsequence specific interactions with DNA, and the extent of specificity is determined by the ratio of the specific to nonspecific equilibrium association constants. Some proteins only bind DNA nonspecifically. Classical examples are histones which play a central role in DNA packaging in the form of chromatin[1] and the HMG-box proteins HMGB-1 and HMGB-2 which are thought to play an important architectural role in nucleoprotein complex assembly.[2] In sequence-specific DNA binding proteins, nonspecific interactions with DNA may serve to enhance the specific association rate constant by reducing the dimensionality of the search by means of one-dimensional diffusion along the DNA.[3]

The dynamic nature of nonspecific protein−DNA interactions renders their biophysical characterization at the atomic level technically challenging. Thus, while many structures of specific protein-DNA complexes have been solved, only a few structures of nonspecific protein−DNA complexes have been determined either by crystallography or NMR, and in each case special efforts had to be made to obtain a unique complex.[4,5] NMR analysis of large-scale dynamics involved in nonspecific protein−DNA interactions has also been very difficult because of the lack of long-range structural information afforded by conven-

[†] National Institute of Diabetes and Digestive and Kidney Diseases, National Institutes of Health.

[‡] Center for Information Technology, National Institutes of Health.

(1) (a) Kornberg, R. D.; Lorch, Y. *Cell* **1999**, *98*, 285−294. (b) Elgin, S. C. R.; Workman, J. L. *Chromatin Structure and Gene Expression*; Oxford University Press: Oxford, 2000.

(2) (a) Bustin, M.; Reeves, R. *Prog. Nucleic Acid Res. Mol. Biol.* **1996**, *54*, 35−100. (b) Bustin, M. *Mol. Cell. Biol.* **1999**, *19*, 5237−5246. (c) Thomas, J. O.; Travers, A. A. *Trends Biochem. Sci.* **2001**, *6*, 167−174. (d) Thomas, J. O. *Biochem. Soc. Trans.* **2001**, *29*, 395−401. (e) Agresti, A.; Bianchi, M. E. *Curr. Opin. Genet. Dev.* **2003**, *13*, 170−178.

(3) (a) von Hippel, P. H.; Berg, O. G. *J. Biol. Chem.* **1989**, *264*, 675−678. (b) Shimamoto, N. *J. Biol. Chem.* **1999**, *274*, 15293−15296. (c) Halford, S. E.; Marko, J. G. *Nucleic Acids Res.* **2004**, *32*, 3040−3052. (d) Zhou, H.-X.; Szabo, A. *Phys. Rev. Lett.* **2004**, in press.

(4) (a) Luger, K.; Mader, A. W.; Richmond, R. K.; Sargent, D. F.; Richmond, T. F. *Nature* **1997**, *389*, 251−260. (b) Agback, P.; Baumann, H.; Knapp, S.; Ladenstein, R.; Härd, R. *Nat. Struct. Biol.* **1998**, *5*, 579−584. (c) Robindson, H.; Gao, Y.-G.; McCray, B. S.; Edmondson, S. P., Shriver, J. W.; Wang, A. H.-J. *Nature* **1998**, *392*, 202−205. (d) Murphy, F. V. IV; Sweet, R. M.; Churchill, M. E. *EMBO J.* **1999**, *18*, 6610−6618. (e) Swinger, K. K.; Lemberg, K. M.; Zhang, Y. A.; Rice, P. A. *EMBO J.* **2003**, *22*, 3749−3760. (f) Kalodimos, C. G.; Biris, N.; Bonvin, A. M.; Levandowski, M. M.; Guennuegues, M.; Boelens, R.; Kaptein, R. *Science* **2004**, *305*, 386−389.

(5) Ohndorf, U.-M.; Rould, M. A.; He, Q.; Pabo, C. O.; Lippard, S. J. *Nature* **1999**, *399*, 708−712.

10.1021/ja046246b

tional NMR methodologies, such as the nuclear Overhauser effect, which are reliant on short (<6 Å) range interactions. In addition, orientational information from residual dipolar couplings[6] is very difficult to interpret in the context of highly dynamic systems.

Long-range distance information (up to ~35 Å), however, can be derived from paramagnetic relaxation enhancement (PRE) which relies on magnetic interactions between unpaired electrons and nuclei.[7] Recently, we described the use of Mn^{2+}-chelated EDTA-derivatized deoxythymidine (dT-EDTA-Mn^{2+}) as an extrinsic paramagnetic probe for the measurement of ^{1}H-PRE data on specific protein−DNA complexes.[8] dT-EDTA[9] provides a tight binding site for a paramagnetic ion and can be introduced at any desired position along the DNA molecule by conventional solid-state synthesis. We showed that the ^{1}H-PRE provides a rapid, qualitative means for assessing protein-binding polarity in specific protein−DNA complexes.[8] Quantitative use of the ^{1}H-PRE in NMR structure refinement is more complex since the EDTA-Mn^{2+} group, which is covalently linked to the thymine base via several rotatable bonds, is intrinsically highly flexible. To this end, we therefore developed an appropriate theoretical framework and computational strategy involving an ensemble representation of the EDTA-Mn^{2+} group and demonstrated that refinement against ^{1}H−PRE data affords significant gains in coordinate accuracy.[10]

In this paper, we demonstrate, using the A-box of the classical nonspecific DNA binding protein HMGB-1 (HMGB-1A) as an example, that ^{1}H-PRE measurements also offer a powerful and unique approach for studying large-scale dynamics associated with nonspecific protein−DNA interactions. HMGB-1 and SRY belong to the same HMG-box family sharing homologous DNA-binding domains (Figure 1A), but whereas the latter binds sequence specifically, the former shows little or no evidence of any sequence preference.[2] HMG-box proteins bind to DNA in the minor groove and induce large-scale DNA bending.[4d,5,11−14] Generally, proteins that bend DNA have enhanced affinity for pre-bent as opposed to linear DNA, which can be rationalized on thermodynamic grounds in terms of the structural similarity between the unbound and bound states of DNA.[15] Accordingly, HMGB-1A binds structure specifically to pre-bent DNA such as cisplatin-modified or UV-damaged DNA.[16] Taking advantage of this enhanced affinity, Ohndorf et al. determined the crystal structure of HMGB-1A complexed to cisplatin-modified DNA.[5] The structure is shown in Figure 1B, together with the NMR structure of the sequence-specific SRY/DNA complex[13] for comparison. We show that the ^1H_N-PRE profiles for the nonspecific HMGB-1A/DNA and specific SRY/DNA complexes are dramatically different, and we demonstrate that the absence of sequence specificity can be directly ascertained from a qualitative interpretation of the data. In addition, we show that a semiquantitative estimate of the distribution of HMGB-1A on the DNA can be derived from the ^1H_N-PRE data using a simple jump model involving multiple overlapping binding sites.

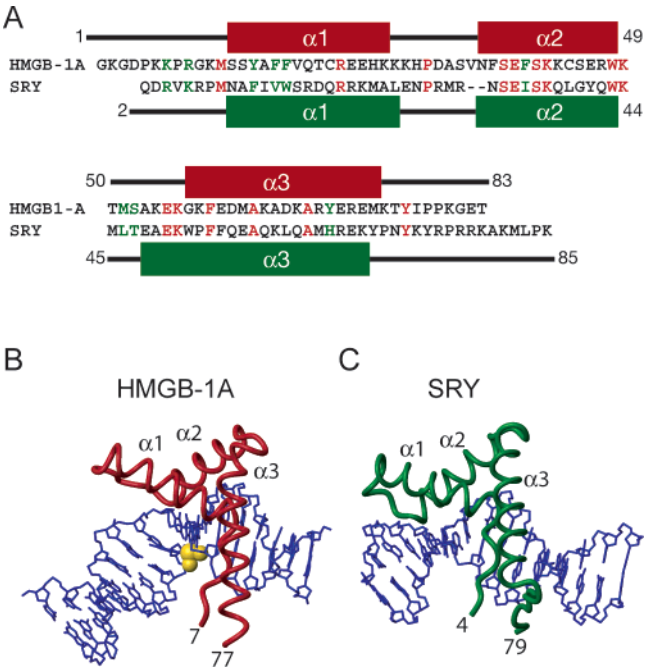

Figure 1. (A) Sequence alignment of the HMG-box DNA binding domains of HMGB-1A and SRY. Identical and similar residues are shown in red and green, respectively. (B) Crystal structure of the complex between HMGB-1A and cisplatin-modified DNA (PDB code: 1CKT).[5] The cisplatin molecule, $Pt(NH_3)_2$, cross-linking two guanine bases is depicted in yellow. HMGB-1A binds specifically to DNA that is pre-bent by cisplatin.[5,16] (C) NMR Structure of the SRY/DNA complex (PDB code: 1J46).[13]

Experimental Section

Preparation of Protein−DNA Complexes. The DNA fragment encoding HMGB-1A (residues 1−84 of HMGB-1) was PCR-amplified using the human HMGB-1 cDNA clone (MGC IMAGE Id 2901382) as a template and subcloned into pET11d. HMGB-1A was expressed in *Escherichia coli* strain BL21(DE3) cultured in minimal medium containing $^{13}C_6$-glucose and $^{15}NH_4Cl$ as the sole carbon and nitrogen sources, respectively. Protein purification was carried out as described previously,[17] and mass spectrometry confirmed the removal of the N-terminal methionine. For consistency with the literature,[5,17] the residue numbering adopted in this paper starts from the second glycine residue. The HMG-box of SRY was expressed and purified exactly as described previously.[13]

Synthetic oligonucleotides were purchased from Midland Certified Reagent Co. Individual strands of DNA (shown in Figures 2 and 3) were purified using anion-exchange (Mono Q) chromatography. After annealing of the complementary strands, the duplex was further purified by anion-exchange chromatography to remove excess single-strand DNA. NMR samples for ^{1}H-PRE meaurements were prepared by mixing the purified protein (^{15}N/^{13}C-labeled) and excess DNA (at natural isotopic abundance) at a molar ratio of 1:1.5 to ensure that all the protein was bound to DNA. The preparation of Ca^{2+}- or Mn^{2+}-chelated states of the complex with DNA containing dT-EDTA was carried out using

(6) Bax, A.; Kontaxis, G.; Tjandra, N. *Methods Enzymol.* **2001**, *339*, 127−174.
(7) Ubbink, M.; Worral, J. A. R.; Canters, G. W.; Groenen, E. J. J.; Huber, M. *Annu. Rev. Biophys. Biomol. Struct.* **2002**, *31*, 393−422.
(8) Iwahara, J.; Anderson, D. E.; Murphy, E. C.; Clore, G. M. *J. Am. Chem. Soc.* **2003**, *125*, 6634−6635.
(9) Dreyer, G. B.; Dervan, P. B. *Proc. Natl. Acad. Sci. U.S.A.* **1985**, *82*, 968−972.
(10) Iwahara, J.; Schwieters, C. D.; Clore, G. M. *J. Am. Chem. Soc.* **2004**, *126*, 5879−5896.
(11) Werner, M. H.; Huth, J. R.; Gronenborn, A. M.; Clore, G. M. *Cell* **1995**, *81*, 705−714.
(12) Love, J. J.; Li, X.; Case, D. A.; Giese, K.; Grosschedl, R.; Wright, P. E. *Nature* **1995**, *376*, 791−795.
(13) Murphy, E. C.; Zhurkin, V. B.; Louis, J. M.; Cornilescu, G.; Clore, G. M. *J. Mol. Biol.* **2001**, *312*, 481−499.
(14) Masse, J. E.; Wong, B.; Yen, Y.-M.; Allain, F. H.-T.; Johnson, R. C.; Feigon, J. *J. Mol. Biol.* **2002**, *323*, 263−294.
(15) McGill, G.; Fisher, D. E. *Chem. Biol.* **1998**, *5*, R29−R38.
(16) (a) Pil, P. M.; Lippard, S. J. *Science* **1992**, *256*, 234−237. (b) Hughes, E. N.; Engelsberg, B. M.; Billings, P. C. *J. Biol. Chem.* **1992**, *267*, 13520−13527. (c) Pasheva, E. A.; Pashev, I. G.; Favre, A. *J. Biol. Chem.* **1998**, *273*, 24730−24736.
(17) Hardmann, C. H.; Broadhurst, R. W.; Raine, A. R. C.; Grasser, K. D.; Thomas, J. O.; Laue, E. D. *Biochemistry* **1995**, *34*, 16596−16607.

the same procedure described previously to ensure complete removal of any excess metal ions.[8] The NMR samples contained 0.3 mM complex in 20 mM Tris-HCl (pH6.8), 20 mM NaCl, 5 mM dithiothreitol (DTT), and 7% D_2O. NMR samples of the SRY-DNA complex[13] used in this study were prepared using exactly the same conditions as those for HMGB-1A.

NMR Experiments. Backbone ^1H, ^{13}C, ^{15}N resonances of HMGB-1A bound to DNA were assigned using three-dimensional triple resonance NMR spectroscopy (3D HNCO, HNCA, HNCACB, CBCA(CO)NH, and ^{15}N-separated NOE spectra)[18] recorded on Bruker DMX-600 or DMX-500 spectrometers equipped with cryogenic *z*-gradient triple resonance probes. Backbone ^1H_N-Γ_2 PRE data arising from Mn^{2+} chelated to the dT-EDTA groups were derived from ^1H_N-T_2 relaxation measurements on the Ca^{2+} and Mn^{2+} chelated states at 600 MHz as described previously.[10] Errors in the ^1H_N-Γ_2 values were estimated as described previously.[10] All experiments were carried out at 35 °C, with the exception of the titration experiments monitoring the DNA imino ^1H resonances (Figure 2C) which were carried out at 25 °C. Although disulfide-bond formation between the two cysteine residues (Cys 22 and 44) of HMGB-1A can occur,[17] we found that the samples remained reduced in the presence of 5 mM DTT for several weeks at 35 °C.

Fluorescence Experiments. All fluorescence experiments were carried out at 25 °C using a Jobin Ybon FluoroMax-3 fluorometer equipped with light polarizers and a Peltier temperature control unit. Three types of fluorophore-labeled DNA duplexes were prepared by combinations of 5′-rhodamine-dCCTGCACAAACACC-3′, 5′-fluorescein-dGGTGTTTGTGCAGG-3′, and their unlabeled counterparts. The sequences of the DNA duplexes are identical and shown in Figure 2A. Fluorophore-labeled single strands were purchased from Midland Certified Reagent Co and duplexes were purified using native polyacrylamide gel electrophoresis. Samples were dissolved in 20 mM Tris HCl, pH6.8, and 20 mM NaCl.

The apparent dissociation constant (K_d^{app}) for the binding of HMGB-1A to the 14-bp rhodamine-labeled DNA duplex was determined by fluorescence anisotropy[19] (excitation at 550 nm and emission at 580 nm) in the presence of various concentrations of HMGB-1A ranging from 0 to 4 μM.

Fluorescence resonance energy-transfer (FRET) efficiency[19] for a pair of fluorescein (donor) and rhodamine (acceptor) labels located at distinct 5′-temini were measured on the free DNA, the HMGB-1A/DNA complex, and the SRY/DNA complex. The emission intensity was corrected by reference to the excitation channel intensity. Fluorescence intensity was determined by subtracting buffer data from the sample data. Experiments were carried out under magic-angle conditions[19] at 25 °C using 20 nM fluorophore-labeled DNA. Proteins were titrated into the solutions until the fraction of bound DNA was saturated (HMGB-1A, ~900 nM; SRY, ~30 nM). Values for the FRET efficiencies were determined according to Lorentz et al.[20] Since the quantum yield of fluorescein conjugated to an oligonucleotide is highly dependent on the surrounding environment,[21] the donor quantum yields were measured on both free DNA and protein−DNA complexes, using DNA labeled with the fluorescein donor only. Free fluorescein dissolved in 0.1 M NaOH was used as the quantum yield standard. The FRET efficiencies (E) for free DNA and the SRY/DNA complex were 0.10 ± 0.01 and 0.21 ± 0.01, respectively; the corresponding values for the donor quantum yield (measured on samples without the acceptor) were 0.19 ± 0.01 and 0.21 ± 0.01, respectively. The FRET efficiencies for the HMGB-1A/DNA complex with 100, 330, and 910 nM HMGB-1A were 0.29 ± 0.01, 0.33 ± 0.01, and 0.35 ± 0.01, respectively, with corresponding values of 0.40 ± 0.02, 0.43 ± 0.02, and 0.45 ± 0.02, respectively, for the donor quantum yield. (A large increase in quantum yield of fluorescein has also been reported for nonspecific interaction of RecA with DNA).[21] The donor−acceptor distance (R_{D-A}) was calculated using $R_{D-A} = (E^{-1} - 1)^{1/6}R_0$, where R_0 is the Föster distance.[19] The values of R_0 were scaled according to $R_0 = R_0^{ref}(\phi_D/\phi_D^{ref})^{1/6}$, in which the superscript "ref" denotes quantities for a reference of the same donor−acceptor pair. Values of $R_0^{ref} = 57.8$ Å and $\phi_D^{ref} = 0.72$ were taken from ref 22.

Back-Calculation of ^1H_N-Γ_2 Rates for Individual Binding States. To estimate the distribution of HMGB-1A binding sites within the 14-bp region shared by the two 16-bp DNA duplexes (shown in Figure 3), a simple model was employed comprising 13 potential intercalation sites for Phe37 of HMGB-1A, allowing two opposite orientations, and with all binding states assumed to have the same overall architecture as the crystal structure of the HMGB-1A/cisplatin-modified DNA (PDB 1CKT).[5] Structural models of the complex for individual binding states and the dT-EDTA-Mn^{2+} ensemble are necessary to back-calculate the ^1H_N-Γ_2 rates for each binding state. To this end, we used the distribution of the Mn^{2+} ion of the dT-EDTA-Mn^{2+} groups determined for the SRY-DNA complex, employing a 10-conformer model for the dT-EDTA-Mn^{2+} groups (coordinates of 100 Mn^{2+} ions from 10 calculations were included).[10] Instead of generating structures for the individual binding states, the DNA in the crystal structure was extended on both sides using a B-type conformation and the Mn^{2+} ensemble was transferred onto a corresponding position to back-calculate the ^1H_N-Γ_2 rates for each binding state. The latter was carried out using a local coordinate system for each nucleotide residue defined by three orthogonal unit vectors $\mathbf{e}_1$, $\mathbf{e}_2$, and $\mathbf{e}_3$ with the origin at C1′, where $\mathbf{e}_1$ is parallel to C1′-N1 (for pyrimidines) or C1′-N9 (for purines) bond, $\mathbf{e}_2$ is a normal vector to the base plane, and $\mathbf{e}_3$ is the vector product $\mathbf{e}_1 \times \mathbf{e}_2$. Values of ^1H_N-Γ_2 rates for the individual binding states were back-calculated using the molecular structure determination package Xplor-NIH[23] according to our previous paper.[10] The overall correlation time $\tau_c = (\tau_r^{-1} + \tau_s^{-1})^{-1}$ was set to 4.8 ns, where τ_r is the rotational correlation time and τ_s is the electron relaxation time. (Calculations were also carried out for values of τ_c ranging from 4 to 6.8 ns to assess the impact of the value of τ_c on the calculated populations). The populations of individual binding states were determined by constrained linear least-squares fitting using linear algebra facilities implemented within the python interface of Xplor-NIH.[23] Only ^1H-PRE data for residues 7−77 were employed since coordinates for the other residues are not present in the crystal structure. The concept behind the population estimations for individual states will be explained in the results section.

Even a semiquantitative analysis of multiple binding state occupancies requires a paramagnetic system with an isotropic *g*-tensor (e.g., Mn^{2+} or a nitroxide spin label). A weaker paramagnetic ion such as Cu^{2+} might appear attractive because the high ^1H-Γ_2 rates arising from Mn^{2+} result in a reduction in experimental sensitivity. However, the use of Cu^{2+} is inappropriate because the electronic *g*-tensor for EDTA-Cu^{2+} is slightly anisotropic ($g_{||} = 2.34$ and $g_\perp = 2.07$; ref 24) which in turn results in pseudo-contact shifts for the observed ^1H nuclei. Although the magnitudes of the pseudo-contact shifts are small, different pseudo-contact shifts for different binding states would result in an additional exchange contribution to the $^1H-T_2$ for the paramagnetic state. Thus, subtraction of the transverse relaxation rate ($1/T_2$) of the diamagnetic state from that for the paramagnetic state would not cancel out this effect, and hence the apparent values of ^1H-Γ_2 would be significantly larger than expected.

(18) (a) Bax, A.; Grzesiek, S. *Acc. Chem. Res.* **1993**, *26*, 131−138. (b) Clore, G. M.; Gronenborn, A. M. *Trends Biotechnol.* **1998**, *16*, 22−34.
(19) Lakowicz, J. R. *Principles of Fluorescence Spectroscopy*, 2nd ed.; Kluwer Academic/Plenum Publishers: New York, 1999.
(20) Lorenz, M.; Hillisch, A.; Goodman, S. D.; Diekmann, S. *Nucleic Acids Res.* **1999**, *27*, 4619−4625.
(21) Sjöback, R.; Nygren, J.; Kubista, M. *Biopolymers* **1998**, *46*, 445−453.
(22) Wang, L.; Gaigalas, A. K.; Blasic, J.; Holden, M. J.; Gallagher, D. T.; Pires, R. *Biopolymers* **2003**, *72*, 401−412.
(23) Schwieters, C. D.; Kuszewski, J.; Tjandra, N.; Clore, G. M. *J. Magn. Reson.* **2003**, *160*, 66−74.
(24) Rojo, T.; Insausti, M.; Lezama, L.; Pizarro, J. L.; Arriortua, M. I.; Calvo, R. *Chem. Soc. Faraday Trans.* **1995**, *91*, 423−426.

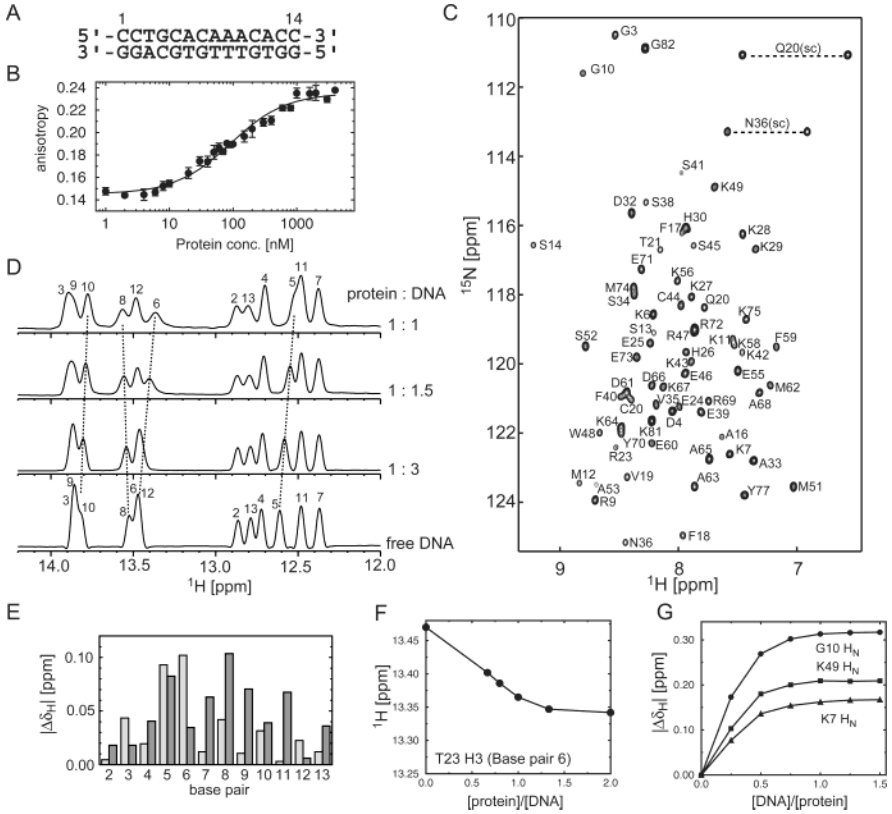

Figure 2. (A) The 14-bp DNA duplex used in the NMR experiments on the HMGB-1A/DNA complex. The identical DNA duplex was used for the structure determination of the SRY/DNA complex.[13] (B) Binding of HMGB-1A to the rhodamine-labeled 14-bp DNA duplex (4 nM) monitored by fluorescence anisotropy. The solid curve, to guide the eye, represents a fit to a simple binding isotherm with an L_{50} of ∼100 nM. This does not take into account statistical factors arising from the fact that there are multiple overlapping binding sites for HMGB-1A on the DNA.[25] (C) ^{1}H−^{15}N HSQC spectrum of the HMGB-1A(^{13}C/^{15}N-labeled)/DNA(unlabeled) complex at a ratio of 1:1.5 protein to DNA to ensure that all protein is bound to DNA and that only a single molecule of protein is bound per 14-bp DNA duplex. (D) Progressive shifts in the DNA imino ^{1}H resonances as a function of protein to DNA ratio. (E) Chemical shift differences of the imino (light gray bars) and cytosine H5 and adenine H2 (dark gray bars) resonances between DNA bound to one molecule of HMGB-1A (ratio of 1:1.5 protein to DNA) and free DNA. (F) Chemical shift changes of the imino proton resonance of T23 (located at base pair 6) as a function of protein to DNA ratio. (G) Chemical shift changes in selected $^{1}H_N$ resonances as a function of DNA to protein ratio. In the titration experiments, the concentration of protein was ∼0.3 mM and the DNA concentration was varied from 0.075 mM to 0.9 mM.

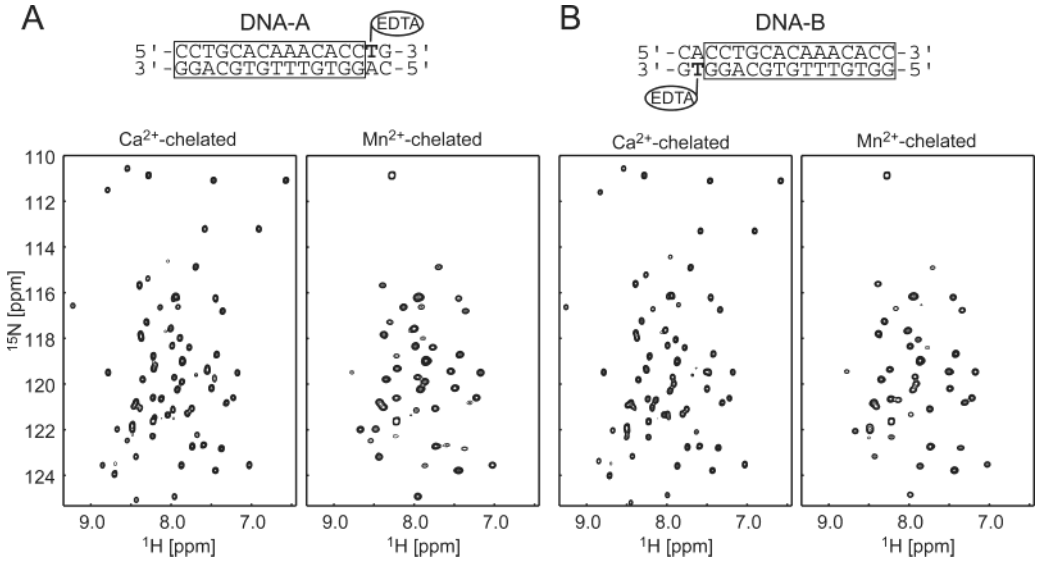

Figure 3. ^{1}H−^{15}N HSQC spectra of HMGB-1A/DNA complexes (1:1.5 ratio of protein to DNA) using 16-bp DNA duplexes with the dT-EDTA group chelating Ca^{2+} or Mn^{2+} located at either the right (A) or left (B) end of the DNA duplex. The two 16-bp duplex oligonucleotides share the same 14-bp sequence (boxed) as that used in Figure 2, and the locations of the dT-EDTA are indicated by the bold T. These dT-EDTA modified DNA duplexes are the same as those used in our previous PRE analysis of the specific SRY-DNA complex.[8,10] The pattern of line broadening and cross-peak disappearance is very similar for the two Mn^{2+} complexes.

Results and Discussion

NMR of the HMGB-1A/DNA Complex. To permit a straightforward comparison, we investigated nonspecific binding of HMGB-1A to the same DNA (Figure 2A) that was used in our previous work on the sequence-specific SRY/DNA complex.[10,13] The apparent equilibrium dissociation constant (K_{diss}^{app}) for the binding of HMGB-1A to the 14bp DNA, determined by fluorescence anisotropy measurements, is approximately 100 nM (Figure 2B). The true value of K_{diss} can be significantly larger owing to statistical effects, since in the context of nonspecific DNA binding, the 14-bp DNA duplex contains multiple overlapping binding sites for HMGB-1A.[25] That this effect is operative is evidenced by marked nonlinearity of a Scratchard plot[25] of the data in Figure 2B (not shown). If the 14-bp DNA can accommodate two molecules of HMGB-1A, K_{diss} is computed to be ~470 nM with a binding site size of 5.3 base pairs which would be consistent with previous isothermal titration calorimetry experiments.[26]

The $^1H-^{15}N$ correlation spectrum of HMGB-1A bound to the 14-bp DNA duplex is well-dispersed and at a molar ratio of 1:1.5 protein to DNA the resonances are fairly narrow (Figure 2C). The chemical shifts of the DNA imino ^1H signals are dependent on the molar ratio of protein to DNA (Figure 2D and F); the same is true of the protein cross peaks in the $^1H-^{15}N$ correlation spectrum (Figure 2G). Both the $^1H-^{15}N$ correlation spectrum of HMGB-1A and the ^1H spectrum of the DNA imino region broadens significantly when the molar ratio of protein to DNA exceeds 1. The titration at high (>100 μM) protein and DNA concentrations reveals several interesting findings. The chemical shift perturbation of the imino proton DNA spectrum (Figure 2E) is ~50% and ~80% complete at molar ratios of protein to DNA of 0.5 and 1, respectively (Figure 2F). In contrast, the chemical shift perturbation of the ^1H_N protein resonances is already 85% complete at a molar ratio of DNA to protein of 0.5 and >99% complete at 1:1 protein to DNA. These results suggest that up to two HMGB-1A molecules can be bound per 14-bp DNA duplex.

The interaction of HMGB-1A with the 14mer duplex under conditions where only a single HMGB1-A molecule is bound per DNA 14mer is fast on the chemical shift scale (Figure 2E–G): the maximum shift difference between bound and free ^1H_N protein resonances is ~400 Hz at a spectrometer frequency of 600 MHz, indicating that the lifetime of the complex under these conditions (given by $\{[DNA_{sites}]k_{on} + k_{off}\}^{-1}$, where $[DNA_{sites}]$ is the concentration of free DNA binding sites, and k_{on} and k_{off} are the association and dissociation rate constants, respectively) is $\ll$0.5 ms.

Since a high-quality $^1H-^{15}N$ correlation spectrum comprising only a single cross-peak per residue is observed for the HMGB-1A/DNA complex under conditions of excess DNA, one could surmise that HMGB-1A interacts with the 14-bp DNA in one of two modes: either (a) HMGB-1A binds to a specific site on the 14-bp DNA or (b) HMGB-1A binds nonsequence specifically to multiple sites and jumps between those states rapidly. Recently, Masse et al. determined the solution structure of a protein–DNA complex of NHP6A, a yeast homologue of HMGB-1.[14] NHP6A, like HMGB-1, is known as a nonsequence-specific DNA binder. According to that study, the NHP6A protein has microsequence selectivity and binds in a single orientation to a unique position within the 15-bp DNA employed. Since HMG-box proteins bend DNA and not all sites in DNA are equally bendable,[27] microsequence selectivity may depend on the bendability of individual DNA sites as well as base-specific contacts. Considering this previous result, one might speculate that model *a* may also be true for HMGB-1A binding to the 14-bp DNA under conditions where the DNA is present in either equimolar amounts or in excess. Model *b*, however, is more consistent with the observation that the chemical shift differences between the DNA protons in the free and bound states of the HMGB-1A complex are significantly smaller than those for the protein amide protons as well as those of the DNA protons in the SRY-DNA complex;[13] if there exist many binding sites in fast exchange, the apparent chemical shift perturbation for the DNA resonances would be expected to be smaller because of cancellation of positive and negative shifts. It is clearly difficult to unambiguously ascertain which model actually holds using conventional NMR techniques.

Nonsequence-Specific DNA Binding Revealed by ^1H_N-Γ_2 Profiles. Backbone ^1H_N-Γ_2 PRE measurements were carried out on HMGB-1A complexed to two 16-bp DNAs with dT-EDTA located at two distinct sites at opposite ends of the DNA duplex: one on the right-hand side of the DNA (Figure 3A), the other on the left (Figure 3B), which we will refer to as DNA-A and DNA-B, respectively. The two 16-bp DNA duplexes share the same 14-bp sequence as the 14-bp DNA used above. The protein-to-DNA ratio employed was 1:1.5 to ensure that all the protein was bound to the DNA and that no more than one protein molecule was bound per 14-bp DNA duplex. The corresponding $^1H-^{15}N$ correlation spectra of HMGB-1A bound to the two 16-bp DNAs with Ca^{2+} or Mn^{2+} chelated to dT-EDTA are also shown in Figure 3A and B, respectively. The $^1H-^{15}N$ correlation spectra for the Ca^{2+}-chelated states are essentially identical to the spectrum of HMGB-1A complexed to the 14-bp DNA. Thus, the DNA-binding mode is unaffected by the presence of an additional two bases including dT-EDTA. For the Mn^{2+}-chelated states, however, cross-peaks in the $^1H-^{15}N$ correlation spectra are differentially broadened because of the PRE effect. The key feature of these spectra is that the pattern of cross-peak broadening is surprisingly similar for the two complexes (cf. Figure 3A and 3B), despite the fact that the positions of the dT-EDTA-Mn^{2+} are located at opposite ends of the DNA duplex. ^1H_N backbone amide resonances of residues 3, 4, 9–16, and 35–41 were broadened beyond detection for both samples in the Mn^{2+}-chelated state. The only explanation for these observations is that HMGB-1A binds nonspecifically to multiple sites on the two 16-bp DNA duplexes. Since both modified oligonucleotides have a dT-EDTA at the second position in from the 3′-terminus, the ^1H_N-PRE profiles for the two complexes should be essentially identical if the DNA-binding properties of HMGB-1A are perfectly nonsequence specific.

The variation in the backbone ^1H_N-Γ_2 rates arising from dT-EDTA-Mn^{2+} as a function of residue is plotted for both 16-bp DNA duplexes in Figure 4A. Data on a negative control lacking

(25) Cantor, C. R.; Schimmel, P. R. *Biophysical Chemistry Part III: The Behavior of Biological Macromolecules;* W. H. Freeman & Co.: San Francisco, CA, 1980; Chapter 15, pp 849–886.
(26) Müller, S.; Bianchi, M. E.; Knapp, S. *Biochemistry* **2001**, *40*, 10254–10261.
(27) (a) Dickerson, R. E. *Nucleic Acids Res.* **1998**, *26*, 1906–1926. (b) Olson, W. K.; Gorin, A.; Lu, X.-J.; Hock, L. M.; Zhurkin, V. B. *Proc. Natl. Acad. Sci. U.S.A.* **1998**, *95*, 11163–11168.

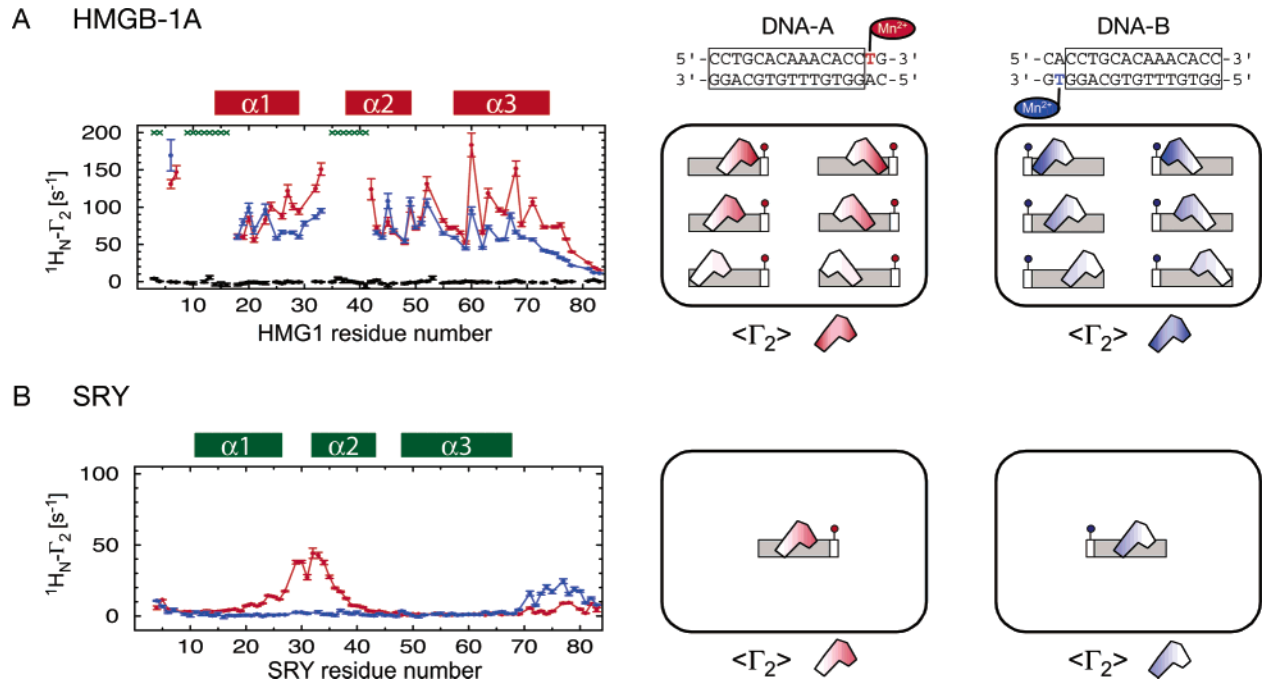

Figure 4. ^1H_N-Γ_2 profiles measured at 600 MHz for (A) the nonspecific HMGB-1A/DNA complex (1:1.5 ratio of protein to DNA) and (B) the specific SRY/DNA complex. The left-hand panels display the ^1H_N-Γ_2 rates arising from the dT-EDTA-Mn^{2+} group located on the right (DNA-A, red) or left (DNA-B, blue) end of the 16-bp DNA duplexes as a function of residue number. The measurements on the HMGB-1A and SRY complexes were carried out under identical conditions using the same DNA fragments. In the HMGB-1A/DNA complex (left-hand panel of A), the green asterisks indicate residues that are broadened beyond detection by the PRE. Also shown in black in the left-hand panel of A are the results of a negative control experiment in which diamagnetic and paramagnetic samples were prepared in the same manner as for the other samples but using the 14-bp DNA duplex without the EDTA-group (shown in Figure 2A). The fact that ^1H_N-Γ_2 rates for the negative control are close to zero indicates that the large values of the ^1H_N-Γ_2 rates for the HMGB-1A/DNA complexes containing Mn^{2+}-chelated to dT-EDTA are not due to undesired Mn^{2+} located at sites other than the conjugated EDTA-group. The vertical bars represent the errors in the measurement (calculated as described in ref 10). The right-hand panels of the figure depict a cartoon representation that explains the observed ^1H_N-Γ_2 data on the two complexes. The two 16-bp oligonucleotides are given above the panels with the site of the EDTA-conjugated T colored in red (DNA-A) and blue (DNA-B). The color gradient within the cartoon representation of the proteins depicts the magnitude of the ^1H-PRE observed with DNA-A and DNA-B, and the location of the Mn^{2+} ion chelated to dT-EDTA is depicted as a red (DNA-A) or blue (DNA-B) circle. In the case of nonspecific binding (i.e. the HMGB-1A/DNA complex), the protein can bind in two orientations differing by 180° at multiple sites on the DNA. The observed ^1H_N-Γ_2 rates are therefore ensemble averages which will be very similar for both oligonucleotides. For the specific SRY/DNA complex, however, the protein is bound at a unique site in a unique orientation, and hence the observed ^1H_N-Γ_2 rates for the two oligonucleotides are very different from one another.

the EDTA unit (shown in black) were also obtained: diamagnetic and paramagnetic samples were prepared in exactly the same way as that for the EDTA-conjugated complexes, but using the previous 14-bp DNA without EDTA conjugation, and the apparent ^1H-Γ_2 rates were measured. The ^1H_N-Γ_2 rates for the negative control are close to zero, indicating that the ^1H-PRE observed for the EDTA-conjugated complexes arises solely from Mn^{2+} chelated to the dT-EDTA-groups. As expected from the $^1H-^{15}N$ correlation spectra of the Mn^{2+}-chelated states of the HMGB-1A/DNA complexes shown in Figure 3, the profiles of ^1H_N-Γ_2 obtained with the two 16-bp DNA duplexes are very similar (Figure 4A). Slight differences, however, are apparent with the ^1H_N-Γ_2 rates for the complex with DNA-A being systematically larger than those with DNA-B. These results indicate that while HMGB-1A binds nonspecifically to multiple sites on the DNA, the affinity for these different sites is not completely uniform.

The results for HMGB-1A are in clear contrast to those obtained under identical experimental conditions for SRY which binds sequence specifically (Figure 4B): the SRY/DNA complex exhibits very different ^1H_N-Γ_2 profiles with DNA-A and DNA-B. The new data obtained at 600 MHz on the SRY/DNA complex are very similar to the previous data at 500 MHz,[8] as expected since ^1H_N-Γ_2 is dominated by the value of the spectral density function at zero frequency.

The ^1H_N-Γ_2 rates for the HMGB-1A/DNA complex are much larger than those for the SRY/DNA complex (cf. Figure 4A and B). This observation also supports the argument that HMGB-1A binds nonspecifically to DNA. Since ^1H-Γ_2 is proportional to the ensemble average $\langle r^{-6}\rangle$, where r is a $Mn^{2+}-{}^1H$ distance, the observed values of ^1H-Γ_2 are largely determined by the minimum distance.[10] Therefore, the presence of binding sites close to the edge of the DNA where dT-EDTA-Mn^{2+} is located increases the observed ^1H-Γ_2 values. The similar ^1H-Γ_2 profiles together with the large values of ^1H_N-Γ_2 observed for the two dT-EDTA-Mn^{2+} conjugated complexes clearly indicate that HMGB-1A binds to multiple sites with multiple orientations even on the short DNA fragments employed in the current experiments.

DNA-Bending by HMGB-1A Assessed by FRET. DNA circularization experiments have demonstrated that HMGB-1A bends DNA,[28] but the sequence-dependence of DNA-bending induced by HMGB-1A is still unknown. Thus, it was not immediately apparent whether the short DNA oligonucleotides used in the ^1H-PRE experiments are actually bent upon binding HMGB-1A. Although DNA-bending for a static system can be precisely analyzed by means of residual dipolar couplings,[13,29]

(28) Stros, M. J. *Biol. Chem.* **1998**, *273*, 10355−10361.
(29) Vermeulen, A.; Zhou, H. J.; Pardi, A. *J. Am. Chem. Soc.* **2000**, *122*, 9638−9647.

the presence of multiple binding modes would hinder such an analysis. We therefore made use of FRET[19] using a fluorophore-labeled 14-bp DNA duplex with the same sequence as that shown in Figure 2A. Fluorescein (donor) and rhodamine (acceptor) were attached through an amino-C_6 linker at the 5′-terminal phosphate group of each oligonucleotide strand. FRET efficiencies were measured for free DNA, the HMGB-1A/DNA complex, and the SRY/DNA complex, and the donor−acceptor distance for each was estimated using the FRET efficiency and quantum yield of the donor (see Experimental Section). The estimated distances were ∼67 Å for the free 14-bp DNA and ∼59 Å for the SRY/DNA complex. The estimated distances for the HMGB-1A/DNA complex under conditions in which the DNA was half-saturated (corresponding to one molecule of HMGB-1A bound per molecule of 14-bp DNA), 80% saturated, and fully saturated (an average of at least two molecules of HMGB-1A bound per molecule of 14-bp DNA) were 61 ± 1, 60 ± 1, and 59 ± 1 Å, respectively. The ratio of the distances measured for free DNA and SRY bound DNA is in good agreement with the three-dimensional structures: the end-to-end distance between the O5′ atoms of the 5′-terminal nucleotides on each strand is 46 Å for fourteen base pairs of B-type DNA, while the corresponding distance in the NMR structure of the SRY/DNA complex (PDB code 1J46) comprising the same 14-bp DNA is 41 Å.[13] From simple modeling, one can deduce that the distance between the O5′ atom and the center of the chromophore can be as large as ∼19 Å depending on the linker conformation so that the FRET distances could be up to ∼38 Å longer than the end-to-end distance between the 5′-terminal O5′ atoms; thus, the distances estimated by FRET, particularly when conformational flexibility of the chromophores is taken into account, seem to be reasonable. Moreover, the fractional decrease (∼12%) in the FRET distance from free DNA to SRY bound DNA is fully consistent with that estimated from the end-to-end O5′−O5′ distance in the actual structures (∼11%). The distances measured by FRET for the HMGB-1A/DNA complex are the result of an ensemble average for the various binding states. However, since the donor−acceptor distance for the HMGB-1A complex is shorter than that for free DNA, bending of the 14-bp DNA by HMGB-1A is clearly indicated by the FRET experiments.

Estimation of the Distribution of HMGB-1A along the DNA. As discussed above, the ^1H_N-Γ_2 profiles clearly indicate that HMGB-1A interacts with multiple sites on the 14-bp DNA duplex and there exists some degree of site preference. In this section, we estimate the distribution of HMGB-1A along the DNA on the basis of the experimental ^1H_N-Γ_2 data. To this end, we assumed that there are N discrete binding states and the transitions between them are significantly slower than the rotational correlation time but fast on the chemical shift time scale. Under these conditions, the spectral density function for a dipole−dipole interaction vector is independent of the transition rates and angles between the vectors of the individual states.[30] Thus, the ensemble average of ^1H_N-Γ_2 is simply given by the weighted average of the individual states:

$$\langle \Gamma_2 \rangle = \sum_{k=1}^{N} \rho_k \Gamma_{2,k} \qquad (1)$$

where ρ_k and $\Gamma_{2,k}$ are the population and ^1H_N-Γ_2 PRE rate, respectively, for state k. Therefore, if values of $\Gamma_{2,k}$ can be calculated from structural models of the individual binding states, it is possible to estimate values of ρ_k by a constrained least-squares fitting procedure that minimizes the function:

$$\chi^2 = \sum_i \frac{\{\Gamma_{2,\mathrm{obs}}(i) - \sum_{k=1}^{N} \rho_k \Gamma_{2,\mathrm{calc},k}(i)\}^2}{\sigma(i)^2} \qquad (2)$$

where i is the index for each data point; $\Gamma_{2,\mathrm{obs}}(i)$, the observed value of ^{1}H-Γ_2; $\Gamma_{2,\mathrm{calc},k}(i)$, the calculated value of ^{1}H-Γ_2 for binding state k; and $\sigma(i)$, the experimental error for $\Gamma_{2,\mathrm{obs}}(i)$.

To estimate the distribution of HMGB1-A along the DNA, we used a simple model comprised of the following features: (a) there are 13 intercalation sites for Phe37 of HMGB1-A[5] in the 14 base pairs shared between the two 16-bp DNA duplexes (Figure 5A); (b) for each individual intercalation site, the protein can adopt two alternative orientations which differ by 180° (Figure 5A); (c) the individual populations of binding sites (ρ_k) in the shared 14-bp region are the same for the two 16-bp DNA duplexes; and (d) the structure of HMGB-1A and the binding mode at the individual sites are the same as those observed in the crystal structure of the HMGB1-A/cisplatin-modified DNA.[5] With regard to the latter, we note that backbone NH residual dipolar couplings measured on free HMGB-1A dissolved in a liquid crystalline medium of phage pf1 fit the crystal structure of the HMGB1-A/cisplatin-modified DNA with a dipolar coupling R-factor[31] of 20.3%, indicating that the structure of free HMGB-1A in solution and in the crystal structure of the complex are essentially the same. This model for nonsequence specific interactions is clearly an oversimplification. For example, the degree of DNA-bending could be dependent on the DNA sequence around the intercalation site.[27] Thus, the values derived for the fractions of individual states represent a semiquantitative rather than quantitative picture of the overall distribution of the HMGB-1A along the DNA.

The resulting populations of the individual binding states along the DNA are displayed in Figure 5. Despite the relatively crude nature of the model, the correlation between observed and calculated values of ^1H_N-Γ_2 is reasonably good with a PRE Q-factor[10] of 0.36 and correlation coefficient of 0.71 (Figure 5B). The observed values of ^1H_N-Γ_2 tend to be systematically larger than the calculated ones, which probably suggests the presence of shorter electron−nucleus distances than those calculated. The estimated populations for the individual binding states are shown in Figure 5C. The most populated regions comprise sites 5−9 which indicates that HMGB-1A spends more time in the center than at the ends of the DNA duplex. Although the overall populations of the two alternative orientations are almost same (49% and 51% for orientations 1 and 2, respectively), the distribution of binding site occupancies appear to be slightly different for orientations 1 and 2, which may reflect a small degree of sequence-dependent orientational preference. For example, it appears that site 9 is preferred by orientation 1 but not by orientation 2 and vice versa for site 5. The site of intercalation of Phe37 is located at the edge of the DNA binding site. Consequently, HMGB-1A can interact with the full length

(30) Brüschweiler, R.; Case, D. A. *Prog. Nucl. Magn. Reson. Spectrosc.* **1994**, *26*, 27−58.
(31) Clore, G. M.; Garrett, D. S. *J. Am. Chem. Soc.* **1999**, *121*, 9008−9012.

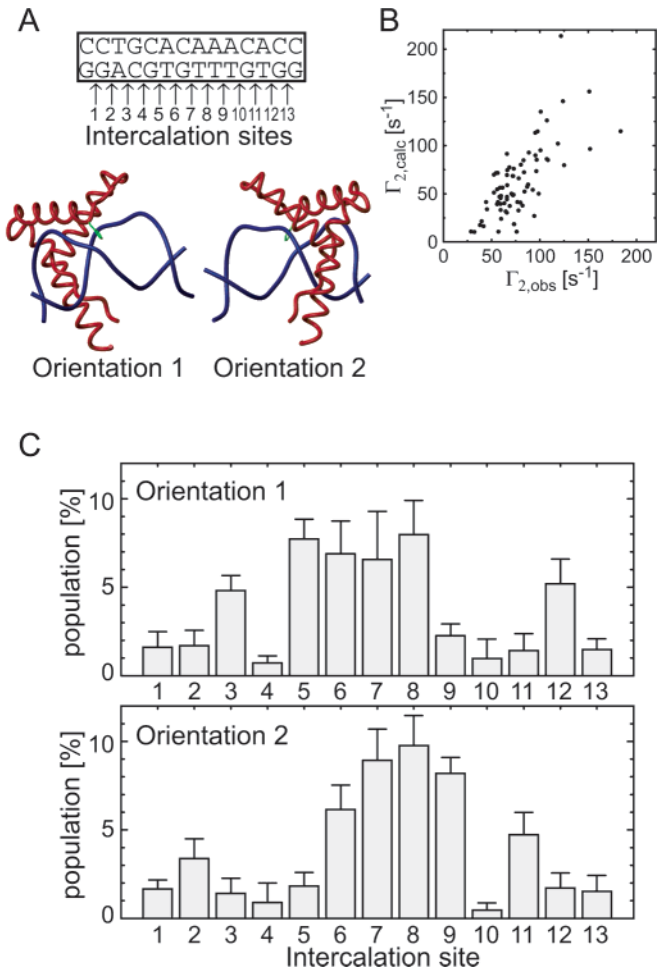

Figure 5. Semiquantitative estimation of the distribution and occupancy of HMGB-1A binding sites along 14-bp duplex DNA. (A) The potential intercalation sites for Phe37 of HMGB-1A are indicated by arrows (top) and the protein can bind to each site in two orientations related by a 180° rotation (bottom). The site of intercalation of Phe37 is located at the edge of the DNA binding site; complete coverage of the DNA binding site (~7 base pairs in the HMGB-1A/cisplatin-modifed DNA complex[5]) by HMGB-1A is obtained at intercalation sites 5−13 in orientation 1 and at intercalation sites 1−9 in orientation 2. (B) Correlation between observed and calculated backbone ^1H_N-Γ_2 rates for HMGB-1A bound to DNA under conditions where one molecule of protein is bound per molecule of DNA (1:1.5 protein-to-DNA ratio). The calculated values of ^1H_N-Γ_2 are ensemble averages defined by eq 1 using the binding models described in the text and the populations derived by constrained linear least-squares analysis using eq 2. The PRE Q-factor[10] and correlation coefficient are 0.36 and 0.71, respectively. (C) Populations of individual binding states in orientations 1 and 2. For simplicity, the overall DNA architecture for the individual binding states was assumed to be the same as that observed in the crystal structure of cisplatin-modified DNA complexed to HMGB-1A.[5] Ten calculations were carried out using different structures in which random deviations were added to the original coordinates with an rms deviation of 1 Å. The values plotted represent the averages and standard deviations for the 10 calculations. Population errors derived from experimental errors of ^{1}H-Γ_2 were roughly 10-times smaller than those derived from 1 Å structural noise. The uncertainties in the populations because of structural noise are comparable to those as a consequence of uncertainty in the exact estimate of the correlation time τ_c (over a range of 4−6.8 ns).

of the DNA binding site (approximately seven base pairs as judged from the crystal structure of the HMGB1-A/cisplatin-modified DNA complex[5]) for intercalations sites 5−13 in orientation 1 and intercalation sites 1−9 in orientation 2. Thus, while one would expect reduced occupancy for intercalation sites 1−4 in orientation 1 and 10−13 in orientation 2, as a consequence of a progressive decrease in protein−DNA contacts, the reduced populations for intercalation sites 9−13 in orientation 1 and intercalation sites 1−5 in orientation 2 must also reflect a small degree of sequence preference (i.e., the population distribution is not the same as one would expect from simple statistical thermodynamic considerations assuming that the interaction energy at any given site is only dependent on the number of base pairs covered by the protein).

Linear One-Dimensional Diffusion of HMGB-1A on DNA and Fast DNA-Bending. The ^{1}H-PRE data indicate that even on a short piece of DNA HMGB1-A binds to multiple sites. The NMR titration experiments show that exchange between free and bound states, as well as any potential jumps between binding states, is fast on the chemical shift time scale. In addition, binding of HMGB-1A to the 14-bp DNA induces DNA bending as evidenced by the FRET experiments. Taking these results together, it seems likely that HMGB-1A may diffuse rapidly along the DNA, bending the DNA on a time scale of micro- or sub-microseconds. This result may at first appear surprising. However, DNA duplex fluctuates by itself on the sub-microsecond time scale, bending its structure transiently,[32] and the flexibility of DNA increases when the negatively charged phosphate backbone is neutralized.[33,34] HMGB-1A may trap a transiently bent site on the DNA in the sub-microsecond to microsecond time regime, diffusing along the DNA strand. Once HMGB-1A binds DNA to a particular site, the adjacent sites may more readily adopt a distorted structure as a consequence of increased DNA flexibility due to charge neutralization and the low dielectric interior of the protein,[35] which could facilitate the protein sliding on the DNA. In intact HMGB-1, the situation could potentially be more complex owing to the presence of two HMG-box domains and an acidic C-terminal tail which is thought to modulate DNA binding.[36] However, the results observed in the current study should provide a good description of nonspecific DNA binding for HMG-box proteins that have only a single HMG-box domain and no basic or acidic extensions. It is also intriguing to note that intact HMGB-1 is the most mobile nuclear protein in living cells, traveling the entire nucleus in less than 1.5 s.[2e]

Concluding Remarks

We have shown that ^{1}H-PRE profiles arising from dT-EDTA-Mn^{2+} groups located at opposite ends of a DNA oligonucleotide duplex provide a unique means to detect and investigate nonspecific protein−DNA interactions. If reasonable structural models for individual binding sites can be generated from available crystal or NMR structures, it is possible to obtain an approximate semiquantitative estimate of the distribution of the protein along the DNA. Although observation of ^{1}H-PREs on DNA in the presence and absence of protein using paramagnetic cosolutes such as 4-hydroxy-TEMPO[37] or Gd-DTPA-BMA[38]

(32) Okonogi, T. M.; Reese, A. W.; Alley, S. C.; Hopkins, P. B.; Robinson, B. H. *Biophys. J.* **1999**, *77*, 3256−3276.
(33) Strauss, J. K.; Maher, L. J., III. *Science* **1994**, *266*, 1829−1834.
(34) Okonogi, T. M.; Alley, S. C.; Harwood, E. A.; Hopkins, P. B.; Robinson, B. H. *Proc. Natl. Acad. Sci. U.S.A.* **2002**, *99*, 4156−4160.
(35) Elcock, A. H.; McCammon, J. A. *J. Am. Chem. Soc.* **1996**, *118*, 3787−3788.
(36) (a) Lee, K-.B.; Thomas, J. O. *J. Mol. Biol.* **2000**, *304*, 135−149. (b) Webb, M.; Payet, D.; Lee, K-.B.; Travers, A. A.; Thomas, J. O. *J. Mol. Biol.* **2001**, *309*, 79−88. (c) Bonaldi, T.; Langst, G.; Strohner, R.; Becker, P. B.; Bianchi, M. E. *EMBO J.* **2002**, *21*, 6865−6873. (d) Jung, Y.; Lippard, S. J. *Biochemistry* **2003**, *42*, 2664−2671.
(37) (a) Petros, A. M.; Mueller, L.; Kopple, K. D. *Biochemistry* **1990**, *29*, 10041−10048. (b) Fesik, S. W.; Gemmecker, G.; Olejniczak, E. T.; Petros, A. M. *J. Am. Chem. Soc.* **1991**, *113*, 7080−7081.

might permit a similar analysis and yield information on which parts of the DNA are shielded by the protein, the method presented in this paper is more straightforward from the perspective of both data collection and its interpretation.

Ascertaining the existence of nonspecific binding does not necessarily require NMR resonance assignments; a simple comparison of the $^{1}H-^{15}N$ correlation spectra spectra of two Mn^{2+}-chelated samples, with the dT-EDTA group located at opposite ends of the duplex, may be sufficient as evidenced by the spectra shown in Figure 2. If the two spectra exhibit severe resonance line broadenings for more residues than expected and the patterns of resonance broadening are similar for the two samples, the presence of nonsequence-specific interactions is clearly indicated. Such qualitative PRE-based characterization might be useful to facilitate the design process of artificial transcription factors.[39]

Acknowledgment. This work was supported in part by the AIDS Targeted Antiviral program of the Office of the Director of the NIH (to G.M.C.).

JA046246B

(38) Pintacuda, G.; Otting, G. *J. Am. Chem. Soc*. **2002**, *124*, 372−373.

(39) Pomerantz, J. L.; Sharp, P. A.; Pabo, C. O. *Science* **1995**, *267*, 93−96.